A high-capacity TiO(2)/C negative electrode for sodium secondary batteries with an ionic liquid electrolyte

Ding, Changsheng; Nohira, Toshiyuki; Hagiwara, Rika

Journal of Materials Chemistry A

COMMUNICATION

High-capacity TiO_2/C negative electrode for sodium secondary battery with ionic liquid electrolyte

Changsheng Ding,[a] Toshiyuki Nohira *[b] and Rika Hagiwara *[a]

Received 00th January 20xx,
Accepted 00th January 20xx

DOI: 10.1039/x0xx00000x

www.rsc.org/

We report TiO_2/C as negative electrode for sodium secondary battery with ionic liquid electrolyte. The TiO_2/C negative electrode delivers 275 mAh g^{-1} of reversible discharge capacity at 10 mA g^{-1} at 363 K. In sodium secondary battery, for the first time, the TiO_2 negative electrode shows a high reversible discharge capacity of large than 250 mAh g^{-1}. In addition, the TiO_2/C negative electrode also exhibits high rate capability and good cycling performance.

Sodium secondary batteries are considered a promising system for the replacement of lithium ion batteries because sodium is less expensive and more abundant than lithium.[1-6] In recent years, a variety of high performance positive electrode materials have been developed for room-temperature sodium secondary batteries.[1,7-11] However, relatively few materials have been reported for the negative electrode. Tin and tin alloys have been demonstrated to have high reversible capacities, but these alloys suffer from low cycling performances due to the large volume changes that occur during charge-discharge cycles.[12,13] Hard carbon materials were used as Na^+ insertion negative electrode materials, which exhibited improved sodium storage capability.[14,15] Unfortunately, hard carbon electrodes tend to exhibit a plateau below 0.1 V vs. Na/Na^+, raising safety concerns for practical applications, because of metallic sodium plating and dendrite formation. Sodium titanium oxides (e.g. $Na_2Ti_3O_7$) have also been investigated as alternative negative electrode materials for sodium secondary batteries, operating at a slightly elevated potential of about 0.3 V vs. Na/Na^+.[16-18]

Recently, titanium dioxide (TiO_2), an attractive alternative negative electrode material to graphite for lithium ion batteries,[19-21] was investigated as the negative electrode material for sodium secondary batteries. However, there are only a few reports on sodium secondary batteries with TiO_2 electrodes. Xiong et al.[22] reported the use of amorphous TiO_2 nanotubes, which were grown directly on titanium thin-foil. These amorphous TiO_2 nanotube electrodes showed a discharge capacity of 75 mAh g^{-1} in the first cycle, and the discharge capacity increased gradually with each charge-discharge cycle. Xu et al.[23] investigated the use of nanocrystalline anatase TiO_2 for sodium secondary batteries. A highly stable and reversible discharge capacity of about 150 mAh g^{-1} was achieved in the first cycle and remained constant for up to about 100 cycles. Huang et al.[24] used TiO_2(B) nanotubes as the negative electrodes in sodium secondary batteries, achieving a discharge capacity of approximately 87 mAh g^{-1} in the initial charge-discharge cycle. Kim et al.[25] investigated anatase TiO_2 nanorods, which were synthesized by a hydrothermal method. The TiO_2 nanorod electrode exhibited a discharge capacity of 193 mAh g^{-1} in the first charge-discharge cycle and displayed a high rate capability and good cycling performance. Wu et al.[26] tested anatase TiO_2 nanoparticles as negative electrode materials, determined the important role of electrolyte composition (salt and solvent), and achieved a discharge capacity of 126 mAh g^{-1} in the first cycle. Finally, Usui et al.[27] investigated Nb-doped rutile TiO_2 as a potential negative electrode material for sodium secondary batteries, achieving a discharge capacity of about 125 mAh g^{-1} in the initial cycle.

All of the above studies were performed in organic electrolytes like $NaClO_4$/propylene carbonate, which are unfavorable for the construction of large-scale batteries due to the hazards of using these volatile and flammable organic electrolytes. In addition to having high energy density, power density, and durability, sodium secondary batteries are safer and operate over a wide temperature range, making them the preferred choice for electric vehicle applications. Ionic liquids are promising alternative electrolytes for sodium secondary batteries, because of their negligibly low volatility, non-flammability, and high thermal and electrochemical stability. Ionic liquids like Na[TFSA]-Cs[TFSA] (TFSA = bis(trifluoromethylsulfonyl)amide)[28], Na[FSA]-K[FSA] (FSA = bis(fluorosulfonyl)amide)[29], and Na[FSA]-[C_3C_1pyrrr][FSA] (C_3C_1pyrr = *N*-methyl-*N*-propylpyrrolidinium)[30] are promising electrolytes for sodium secondary batteries, because of their good electrochemical

[a] Graduate School of Energy Science, Kyoto University, Sakyo-ku, Kyoto 606-8501, Japan. E-mail: hagiwara@energy.kyoto-u.ac.jp; Tel.: +81-75-753-5822; Fax: +81-75-753-5906
[b] Institute of Advanced Energy, Kyoto University, Uji 611-0011, Japan. E-mail: nohira.toshiyuki.8r@kyoto-u.ac.jp

Electronic Supplementary Information (ESI) available. See
DOI: 10.1039/x0xx00000x

performance. Na[FSA]-[C_3C_1pyrrr][FSA] is an especially attractive electrolyte candidate, because of its wide operating temperature range.[30] In this work, the electrochemical performance of carbon-coated anatase TiO_2 (TiO_2/C) nanopowders is determined in sodium half cells using Na[FSA]-[C_3C_1pyrrr][FSA] ionic liquid as the electrolyte. The TiO_2/C negative electrode has a high discharge capacity of 275 mAh g^{-1} at 10 mA g^{-1} in the first cycle and exhibits a high rate capability and improved cycling performance at 363 K.

The TiO_2/C nanopowders were prepared by coating citric acid on commercial anatase TiO_2 nanopowders and performing heat treatment in an Ar atmosphere. Figure 1a shows the X-ray diffraction (XRD) patterns of the TiO_2 and TiO_2/C nanopowders. All of the diffraction peaks can be indexed to anatase TiO_2 phase (JCPDS file No. 01-084-1285), suggesting that the carbon coating does not alter the original anatase TiO_2 crystal structure. The field emission scanning electron microscopy (FE-SEM) image (Figure 1b) reveals that the TiO_2/C nanopowders have a uniform size distribution and particle sizes of about 50-100 nm. The carbon content in the TiO_2/C nanopowders was determined to be approximately 3.0 wt%, as confirmed using a CHN analyzer. According to the transmission electron microscopy (TEM) observation, the thickness of carbon layer on the surface of TiO_2/C nanopowders is approximately 2 nm (SI, Figure S1).

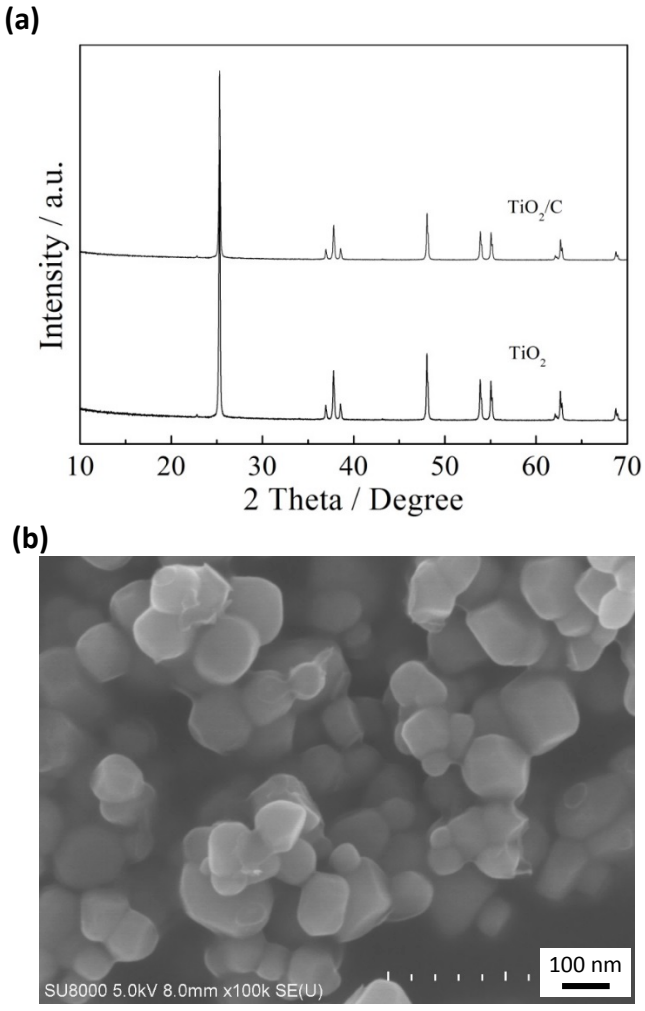

Fig. 1 (a) XRD patterns of TiO_2 and TiO_2/C nanopowders and (b) SEM image of TiO_2/C nanopowders.

The electrochemical performance of the TiO_2/C nanopowders was evaluated at 363 K in sodium half cells using Na metal as the counter electrode and Na[FSA]-[C_3C_1pyrrr][FSA] ionic liquid as the electrolyte. Figure 2a shows cyclic voltammetry (CV) curves produced by a TiO_2/C electrode at a scan rate of 0.1 mV s^{-1} in the voltage range of 0-2.5 V. In the first cycle, the reduction (Na intercalation) process consists of two peaks. The reduction peak at around 1.25 V is attributable to side-reactions including electrolyte reduction and the formation of a solid-electrolyte interphase (SEI)[23,26], which have also been observed for layered sodium titanates[16,18,31]. The reduction peak at around 0.15 V is attributable to the insertion of Na into the TiO_2/C and further decomposition of the electrolyte. Upon subsequent cycling, the reduction peak at 1.25 V vanishes, while the reduction peak at 0.15 V diminishes and shifts to 0.5 V. The oxidation (Na de-intercalation) process has a broader peak near 0.75 V, which does not change with cycle number.

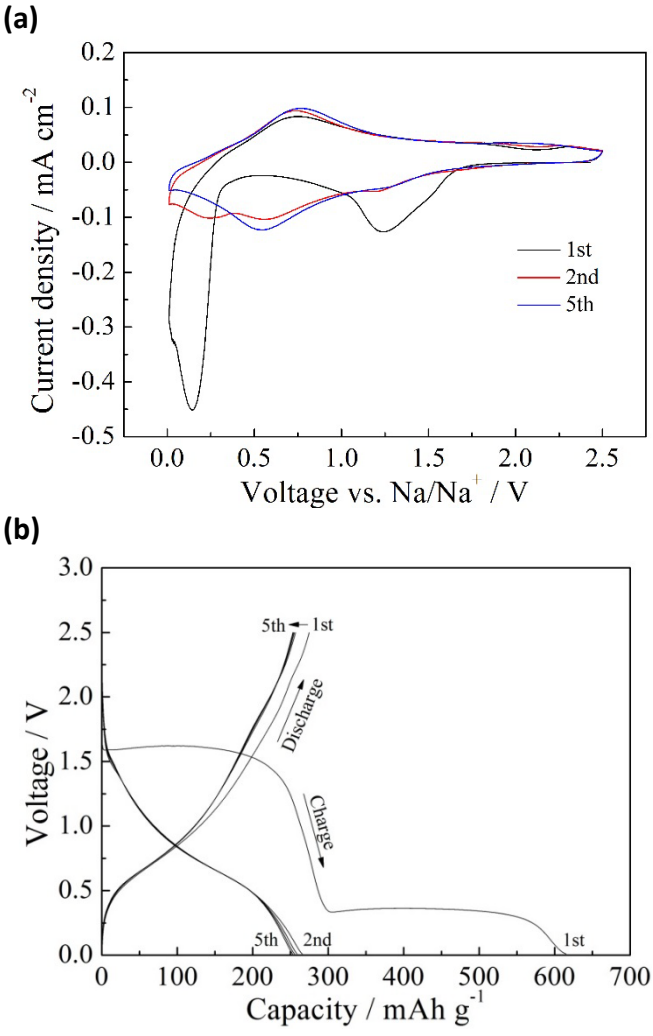

Fig. 2 (a) Cyclic voltammograms of a TiO_2/C electrode recorded at a scan rate of 0.1 mV s^{-1}; and (b) Charge-discharge curves of TiO_2/C electrode at current rate of 10 mA g^{-1}.

Figure 2b shows the charge-discharge curves of the TiO_2/C electrode at a current rate of 10 mA g^{-1} in the voltage range of 0.01-2.5 V at 363 K. In the first cycle, the TiO_2/C electrode shows a large charge capacity of 615 mAh $(g\text{-}TiO_2/C)^{-1}$, which is larger than its theoretical capacity of 335 mAh g^{-1}. The voltage profile exhibits two distinct plateaus in the voltage ranges of 1.6 to 1.5 V and 0.4 to 0.3 V. These voltage plateaus are in agreement with observations in the CV curves. The first discharge capacity achieved is 275 mAh g^{-1}, indicating a large irreversible capacity greater than 340 mAh g^{-1} with a low coulombic efficiency of 45%. The large irreversible capacity may be attributed to side reactions like electrolyte reduction and SEI formation. To verify the existence of side reactions, TiO_2/C electrodes were charged-discharged at different cut-off voltages of 0.01-2.5, 0.25-2.5, and 0.4-2.5 V (SI, Figure S2). Results indicate that the reversible discharge capacity is 213 mAh g^{-1} in the voltage range of 0.25-2.5 V and decreases to 18 mAh g^{-1} in the voltage range of 0.4-2.5 V. This decrease in discharge capacity indicates that side reactions like electrolyte reduction and SEI formation occur mainly at voltages above 0.4 V in the first cycle, while sodium insertion into the TiO_2/C electrode occurs mainly at the voltage plateau at 0.4-0.3 V. Therefore, the reversible capacity originates mainly from the sodium titanium oxide that is formed by sodium insertion during the first charge process. Similarly, Li insertion into the anatase TiO_2 forms orthorhombic $Li_{0.5}TiO_2$ in Li-ion batteries.[32-34] However, Kim et al. did not observe $Na_{0.5}TiO_2$ formation in anatase TiO_2 electrodes for sodium secondary batteries, but they instead observed the reduction of Ti^{4+} to Ti^{3+} upon sodium insertion.[25] Wu et al. proposed a new reaction mechanism for the anatase TiO_2 negative electrode, including the formation of a sodium titanate phase, metallic titanium, sodium superoxide, and oxygen.[35] The sodium insertion mechanism in anatase TiO_2 remains unclear, especially in ionic liquid electrolytes, which produce different charge-discharge curves. A detailed study on the sodium insertion mechanism in anatase TiO_2 in Na[FSA]-[C_3C_1pyrrr][FSA] ionic liquid is ongoing, and results will be reported in the future.

After the first charge-discharge cycle, the TiO_2/C electrode shows stable cycling behavior with a reversible discharge capacity of approximately 256 mAh g^{-1}. The coulombic efficiency is 97% in the second cycle, and is higher than 99% after 3 cycles. The reversible discharge capacity is higher than those reported for other TiO_2 negative electrode materials used for sodium secondary batteries with organic electrolytes at room temperature including TiO_2 nanoparticles (150 mAh g^{-1} at 40 mA g^{-1}) [26], TiO_2 nanorods (193 mAh g^{-1} at 10 mA g^{-1}) [25], and TiO_2 nanocrystals (170 mAh g^{-1} at 50 mA g^{-1}).[23] For comparison, the charge-discharge testing was also performed at 298 K in Na[FSA]-[C_3C_1pyrrr][FSA] ionic liquid and organic electrolyte (1 M $NaPF_6$ in ethylene carbonate/dimethyl carbonate (EC-DMC, 1:1 in volume)) after high temperature testing, and the results are shown in Figure S3. A reversible discharge capacity of 143 mAh g^{-1} is obtained in the ionic liquid at 298 K. Due to the increased viscosity and decreased conductivity of ionic liquid at 298 K, the discharge capacity is fairly lower than that at 363 K. It is confirmed that high operation temperature largely increases the reversible discharge capacity in the ionic liquid. In the organic electrolyte, the reversible discharge capacity is 114 mAh g^{-1} at 298 K, which is lower than those reported in the literatures[23, 25, 26]. The low discharge capacity may be attributed to the different binder and conductive agent. The polyamide-imide binder used in the present study may not be suitable for application in organic electrolytes. In

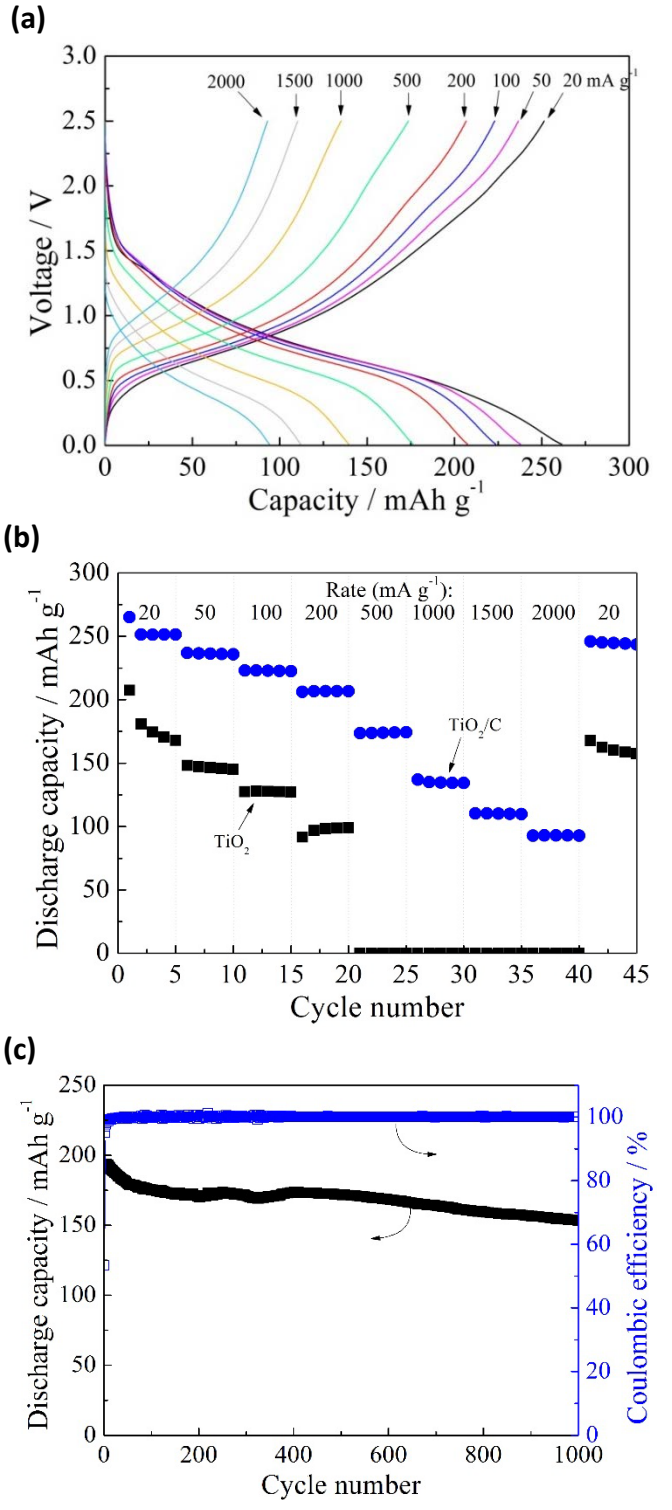

Fig. 3 (a) Charge-discharge curves of a TiO_2/C electrode at current rates of 20-2000 mA g^{-1}; (b) Comparison of rate capability for TiO_2/C and TiO_2 electrodes; and (c) Cycling performance of TiO_2/C electrode at current rate of 200 mA g^{-1}.

order to obtain high discharge capacity in organic electrolytes, one should probably use polyvinylidene fluoride as a binder and carbon black as a conductive agent in preparing the TiO_2/C electrodes.[23, 25] The reversible discharge capacity of TiO_2/C electrode at 363 K is also higher than those of the $Na_2Ti_3O_7$ negative electrodes (170-190 mAh g^{-1})[16-18] used in sodium secondary batteries. In addition, the reversible discharge capacity of the TiO_2/C negative electrode is comparable to that of a hard carbon negative electrode (260 mAh g^{-1}) [36] in Na[FSA]-[C_3C_1pyrrr][FSA] electrolyte, suggesting that TiO_2/C nanopowders are a promising negative electrode material for sodium secondary batteries.

Rate capability is another important parameter describing the performance of sodium secondary batteries. Figure 3a shows the charge-discharge curves of a TiO_2/C electrode at current rates of 20-2000 mA g^{-1} at 363 K. When the charge-discharge current rate is increased, the shapes of the charge-discharge curves remain unchanged. The discharge capacities, however, decrease gradually with an increase in the current rate. Figure 3b shows the rate capability of the TiO_2/C electrode at 363 K. For comparison, the rate capability of the TiO_2 electrode without carbon coating was also measured under the same conditions (SI, Figure S4 and Figure 3b). The TiO_2 negative electrode shows a reversible discharge capacityof approximately 201 mAh g^{-1} at a current rate of 20 mA g^{-1} in the first cycle, which is lower than that of the TiO_2/C electrode. The TiO_2/C electrode shows reversible discharge capacities of 174 and 93 mAh g^{-1} at current rates of 500 and 2000 mA g^{-1}, respectively, which correspond to about 69% and 37% of the capacity at 20 mA g^{-1}. However, the TiO_2 electrode shows a poor rate capability and has a very low discharge capacity (almost 0 mAh g^{-1}) at current rates greater than 500 mA g^{-1} (Figure 3b). Electrochemical impedance spectroscopy (EIS) analysis was conducted for TiO_2/C and TiO_2 electrodes before and after charge-discharge testing (SI, Figure S5). Before the testing, the charge-transfer resistance for the TiO_2/C electrode (ca. 25 Ω) is much lower than that for the TiO_2 electrode (ca. 6000 Ω). Although the charge-transfer resistances both for the TiO_2/C and TiO_2 electrodes increase after the testing, the value for TiO_2/C electrode still remains as low as approximately 85 Ω. Clearly, the carbon coating on the TiO_2/C electrode significantly improves its rate capability.

In order to test cycling performance, a sodium half-cell using the TiO_2/C electrode was operated at a current rate of 200 mA g^{-1} for 1000 cycles at 363 K. Figure 3c shows the cycling performance of the TiO_2/C electrode. In the first cycle, the TiO_2/C electrode shows a discharge capacity of 193 mAh g^{-1} with a coulombic efficiency of 53% due to the irreversible side reactions described previously. After 400 cycles, the discharge capacity remains at 174 mAh g^{-1}, a 10% drop in capacity. After 1000 cycles, the capacity decreases by about 21%. In comparison, the TiO_2 electrode had a discharge capacity of only 73 mAh g^{-1} after 1000 cycles, representing a capacity loss of about 42% (SI, Figure S6). These results indicate that the cycling performance of the TiO_2/C electrode is superior to that of the TiO_2 electrode.

Conclusions

In summary, carbon-coated anatase TiO_2 nanopowders (TiO_2/C) were synthesized, and their electrochemical performance as negative electrode materials for sodium secondary batteries using a Na[FSA]-[C_3C_1pyrr][FSA] ionic liquid electrolyte was evaluated. The TiO_2/C negative electrode displayed a reversible discharge capacity of 275 mAh g^{-1} at a current rate of 10 mA g^{-1}, which is higher than those reported in previous work. In addition, the TiO_2/C negative electrode also exhibits a higher rate capability and better cycling performance compared to a TiO_2 electrode without a carbon coating. The discharge capacity of the TiO_2/C electrode is comparable to that of hard carbon electrodes operated in the same Na[FSA]-[C_3C_1pyrr][FSA] ionic liquid electrolyte, suggesting that the TiO_2/C nanopowders are an attractive candidate for the negative electrode material in ionic liquid-based sodium secondary batteries.

Experimental

Commercial anatase TiO_2 nanopowders (SIGMA ALDRICH) were used as raw materials, and citric acid was used as a carbon source to prepare carbon-coated TiO_2 (TiO_2/C) nanopowders. First, citric acid was dissolved in ethanol. The anatase TiO_2 nanopowders were then dispersed in the citric acid solution by stirring. The mixture was then dried at 333 K and heated in an Ar atmosphere at 873 K for 12 h. The structure and morphology of the TiO_2 and TiO_2/C nanopowders were investigated by means of X-ray diffraction (XRD, Rigaku SmartLab) and field emission scanning electron microscopy (FE-SEM, Hitachi SU8000).

Electrochemical characterization was performed using a coin-type 2032 cell with a sodium foil counter electrode. Working electrodes were fabricated using a conventional coating method. A slurry consisting of active material (80 wt%), graphite (15 wt%), and polyamide-imide (5 wt%) in *N*-methyl-2-pyrrolidone (NMP) was uniformly spread onto an Al foil. The mass loading of active material was 1-2 mg cm^{-2}. The packing density of TiO_2/C electrode was approximately 550 mg cm^{-3}. The electrodes were dried in vacuum at 393 K overnight before being transferred into an Ar-filled glove box. The electrolyte used was the Na[FSA]-[C_3C_1pyrr][FSA] ionic liquid with molar ratio of 2:8.[26] A glass fiber filter (Whatman, GF-A, 260 mm) was used as a separator. The working electrodes and separators were vacuum-impregnated with Na[FSA]-[C_3C_1pyrr][FSA] at 333 K before assembling the cells. Charge-discharge tests were conducted at constant current rates of 10 – 2000 mA g^{-1} in the voltage range of 0.01 – 2.5 V at 363 K. For comparison, commercial anatase TiO_2 nanopowders without carbon coating were also studied under the same conditions.

Acknowledgements

This study was partly supported by the Advanced Low Carbon Technology Research and Development Program (ALCA, No. 3428) of the Japan Science and Technology Agency (JST) and the “Elements Strategy Initiative to Form Core Research Center" program of the Japanese Ministry of Education, Culture, Sports, Science and Technology (MEXT).

Notes and references

1 N. Yabuuchi, M. Kajiyama, J. Iwatate, H. Nishikawa, S. Hitomi, R. Okuyama, R. Usui, Y. Yamada, S. Komaba, *Nature Mater*., 2012, **11**, 512-517.
2 D. Kim, E. Lee, C. S. Johnson, *Adv. Funct. Mater*., 2013, **23**, 947-958.
3 B. L. Ellis, L. F. Nazar, *Curr. Opin. Solid State Mater. Sci*., 2012, **16**, 168-177.
4 X.S. Zhou, X. Liu, Y. Xu, Y.X. Liu, Z.H. Dai, J.C. Bao, *J. Phys. Chem. C*, 2014, **118**, 23527−23534.
5 Y.C. Du, X.S. Zhu, X.S. Zhou, L.Y. Hu, Z.H. Dai, J.C. Bao, *J. Mater. Chem. A*, 2015, **3**, 6787–6791.
6 X.S. Zhou, X.H. Zhu, X. Liu, Y. Xu, Y.X. Liu, Z.H. Dai, J.C. Bao, *J. Phys. Chem. C*, 2014, **118**, 22426−22431.
7 S. Tepavcevic, H. Xiong, V.R. Stamenkovic, X. Zuo, M. Balasubramanian, V.B. Prakapenka, C.S. Johnson, T. Rajh, *ACS Nano*, 2012, **6**, 530-538.
8 S.W. Kim, D.H. Seo, X.H. Ma, G. Ceder, K. Kang, *Adv. Energy Mater.,* 2012**, 2**, 710-721.
9 A. Langrock, Y.H. Xu, Y.H. Liu, S. Ehrman, A. Manivannan, C.S. Wang, *J. Power Sources,* 2013, **223**, 62-67.
10 P. Barpanda, G.D. Liu, C.D. Ling, M. Tamaru, M. Avdeev, S.C. Chung, Y. Yamada, A. Yamada, *Chem. Mater.,* 2013, **25**, 3480-3487.
11 J. Billaud, G. Singh, A. R. Armstrong, E. Gonzalo, V. Roddatis, M. Armand, T. Rojo, P.G. Bruce, *Energy Environ. Sci.,* 2014, **7**, 1387-1391.
12 J.W. Wang, X.H. Liu, S.X. Mao, J.Y. Huang, *Nano Lett.,* 2012, **12**, 5897-5902.
13 T. Yamamoto, T. Nohira, R. Hagiwara, A. Fukunaga, S. Sakai, K. Nitta, S. Inazawa, *J. Power Sources,* 2012, **217,** 479-484.
14 S. Komaba, W. Murata, T. Ishikawa, N. Yabuuchi, T. Ozeki, T. Nakayama, A. Ogata, K. Gotoh, K. Fujiwara, *Adv. Funct. Mater.,* 2011, **21**, 3859-3867.
15 R.S. Babu, M. Pyo, *J. Electrochem. Soc.,* 2014, **161**, A1045-A1050.
16 H. Pan, X. Lu, X.Q. Yu, Y.S. Hu, H. Li, X.Q. Yang, L.Q. Chem, *Adv. Energy Mater.,* 2013, **3**, 1186-1194.
17 P. Senguttuvan, G. Rousse, V. Seznec, J.M. Tarascon, M.R. Palacin, *Chem. Mater*., 2011, **23**, 4109-4111.
18 A. Rudola, K. Saravanan, C.W. Mason, P. Balaya, *J. Mater. Chem. A,* 2013, **1**, 2653-2662.
19 H. Liu, Z.H. Bi, X.G. Sun, R.R. Unocic, M.P. Paranthaman, S. Dai, G.M. Brown, *Adv. Mater.,* 2011, **23**, 3450-3454.
20 D. Deng, M.G. Kim, J.Y. Lee, J. Cho, *Energy Environ. Sci.,* 2009, **2**, 818-837.
21 S.H. Liu, H.P. Jia, L. Han, J.L. Wang, P.F. Gao, D.D. Xu, J. Yang, S.N. Che, *Adv. Mater.,* 2012, **24**, 3201-3224.
22 H. Xiong, M.D. Slater, M. Balasubramanian, C.S. Johnson, T. Rajh, *J. Phys. Chem. Lett.,* 2011, **2**, 2560-2565.
23 Y. Xu, E.M. Lotfabad, H.L. Wang, B. Farbod, Z.W. Xu, A. Kohandehghan, D. Mitlin, *Chem. Commun.,* 2013, **49**, 8973-8975.
24 J.P. Huang, D.D. Yuan, H.Z. Zhang, Y.L. Cao, G.R. Li, H.X. Yang, X.P. Gao, *RSC Adv.,* 2013, **3**, 12593-12597.
25 K.T. Kim, G. Ali, K.Y. Chung, C.S. Yoon, H. Yashiro, Y.K. Sun, J. Lu, K. Amine, S.T. Myung, *Nano Lett.,* 2014, **14**, 416-422.
26 L.M. Wu, D. Buchholz, D. Bresser, L.G. Chagas, S. Passerini, *J. Power Sources,* 2014, **251**, 379-385.
27 H. Usui, S. Yoshioka, K. Wasada, M. Shimizu, H. Sakaguchi, *ACS Appl. Mater. Interfaces,* 2015, **7**, 6567-6573.
28 T. Nohira, T. Ishibashi, R. Hagiwara, *J. Power Sources,* 2012, **205**, 506-509.
29 A. Fukunaga, T. Nohira, Y. Kozawa, R. Hagiwara, S. Sakai, K. Nitta, S. Inazawa, *J. Power Sources,* 2012, **209**, 52-56.
30 C.S. Ding, T. Nohira, K. Kuroda, R. Hagiwara, A. Fukunaga, S. Sakai, K. Nitta, S. Inazawa, *J. Power Sources,* 2013, **238**, 296-300.
31 M. Shirpour, J. Cabana, M. Doeff, *Energy Environ. Sci.,* 2013, **6**, 2538-2547.
32 E. Baudrin, S. Cassaignon, M. Koelsch, J.P. Jolivet, L. Dupont, J.M. Tarascon, *Electrochem. Commun.,* 2007, **9**, 337-342.
33 G. Sudant, E. Baudrin, D. Larcher, J.M. Tarascon, *J. Mater. Chem.,* 2005, **15**, 1263-1269.
34 R. Van de Krol, A. Goossens, E.A. Meulenkamp, *J. Electrochem. Soc.,* 1999, **146**, 3150-3154.
35 L. Wu, D. Bresser, D. Buchholz, G. Giffin, C.R. Castro, A. Ochel, S. Passerini, *Adv. Energy Mater.,* 2015, **5**, 1401142.
36 A. Fukunaga, T. Nohira,R. Hagiwara,K. Numata, E. Itani, S. Sakai, K. Nitta, S. Inazawa, *J. Power Sources,* 2014, **246**, 387-391.

Electronic Supplementary Material (ESI) for Journal of Materials Chemistry A.

Supporting Information

High-capacity TiO_2/C negative electrode for sodium secondary battery with ionic liquid electrolyte

Changsheng Ding[a], *Toshiyuki Nohira**[b] *and Rika Hagiwara**[a]

[a] Graduate School of Energy Science, Kyoto University, Sakyo-ku, Kyoto 606-8501, Japan.
E-mail: hagiwara@energy.kyoto-u.ac.jp; Tel.: +81-75-753-5822; Fax: +81-75-753-5906
[b] Institute of Advanced Energy, Kyoto University, Uji 611-0011, Japan.
E-mail: nohira.toshiyuki.8r@kyoto-u.ac.jp

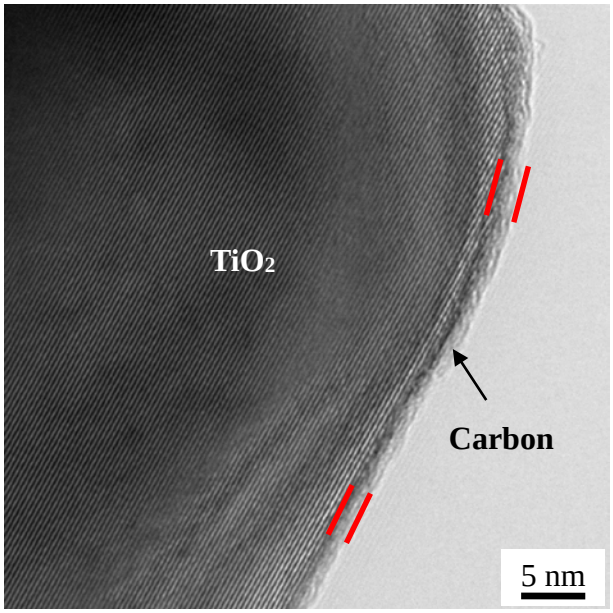

Figure S1. A TEM image of TiO_2/C nanopowder.

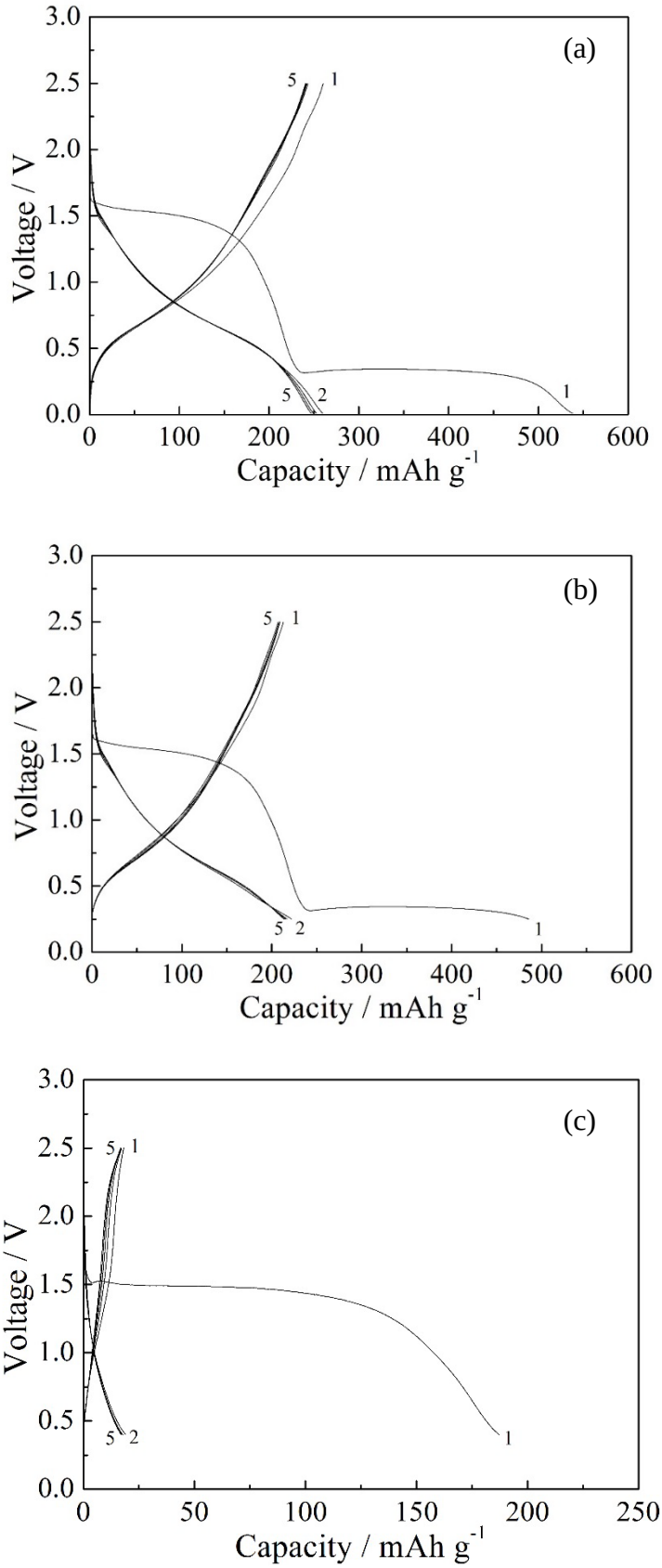

Figure S2. Charge-discharge curves of TiO_2/C electrodes at current rate of 20 mA g^{-1} at 363 K. Cut-off voltage: (a) 0.01-2.5 V, (b) 0.25-2.5 V and (c) 0.4-2.5 V.

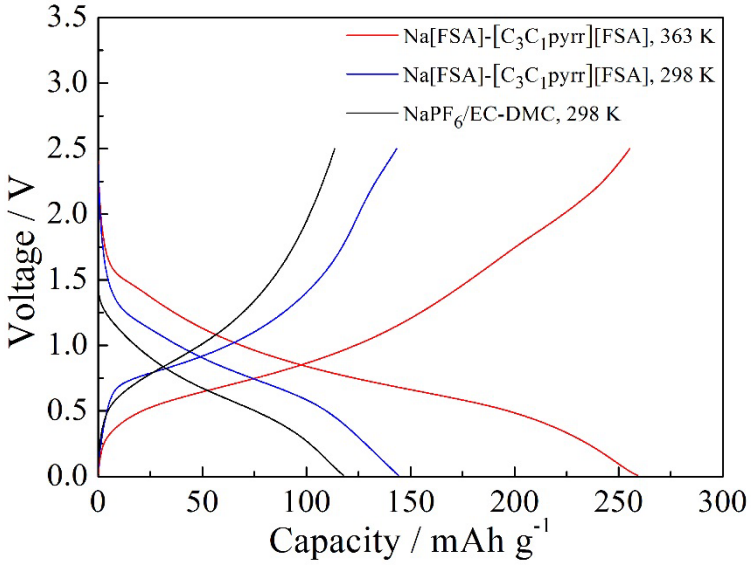

Figure S3. Charge-discharge curves of TiO_2/C electrode in Na[FSA]-[C_3C_1pyrrr][FSA] at 363 K and 298 K, and in 1M-$NaPF_6$/EC-DMC at 298 K. Current rate: 10 mA g^{-1}.

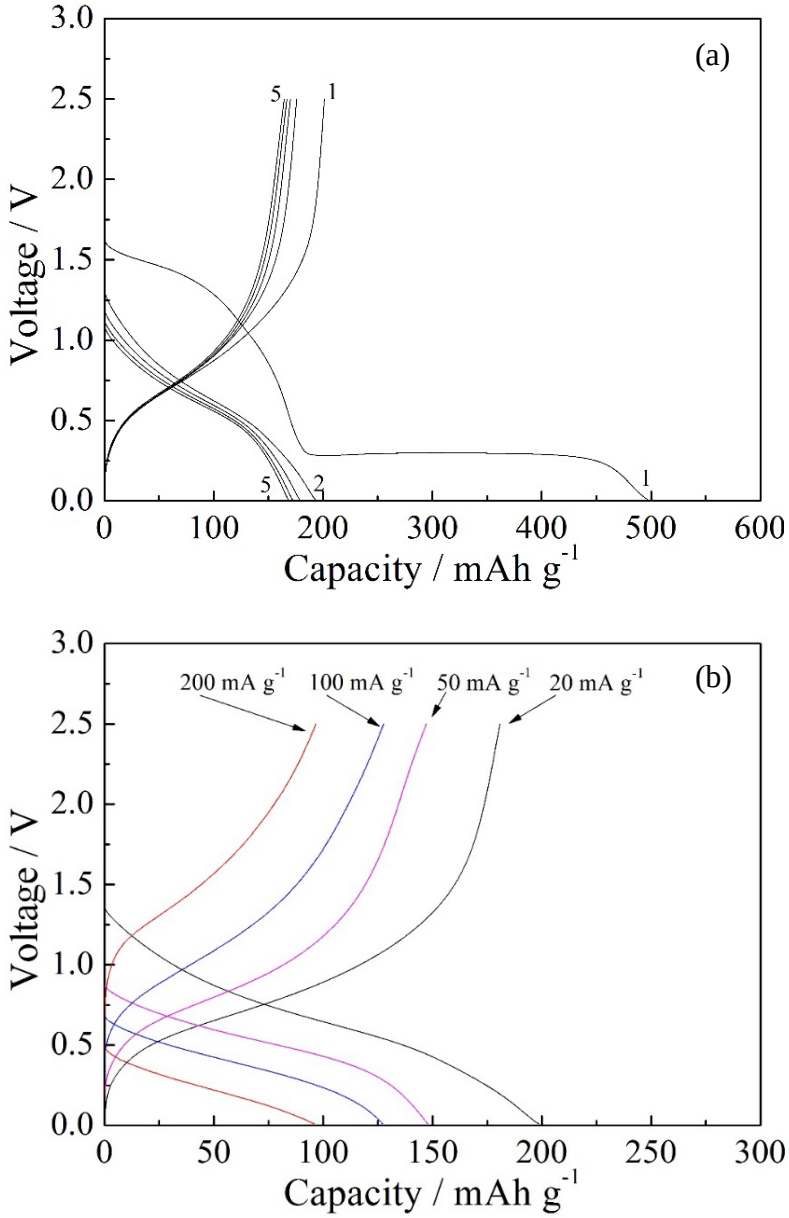

Figure S4. Charge-discharge curves of TiO_2 electrode at 363 K: (a) at current rate of 20 mA g^{-1} and (b) at current rates of 20-200 mA g^{-1}.

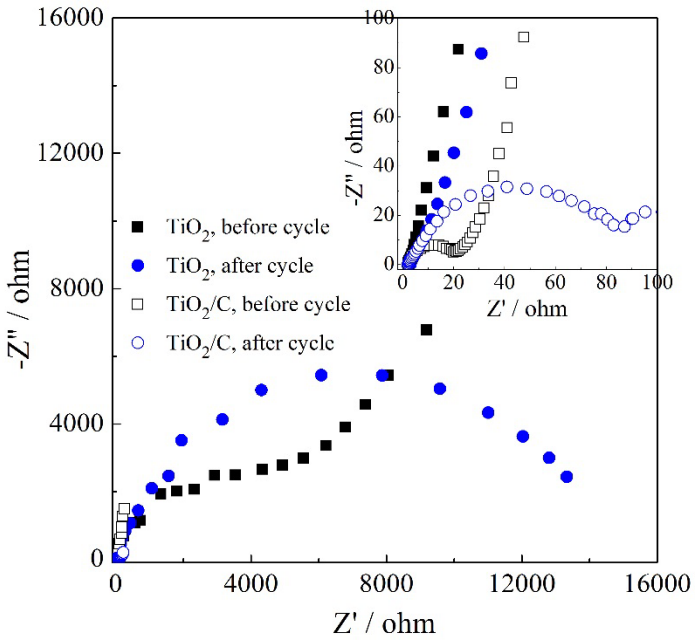

Figure S5. Nyquist plots of TiO_2 and TiO_2/C electrodes before and after charge-discharge testing. (Electrochemical impedance measurements were performed in the frequency range of 200 kHz to 100 mHz with an AC voltage signal of 10 mV)

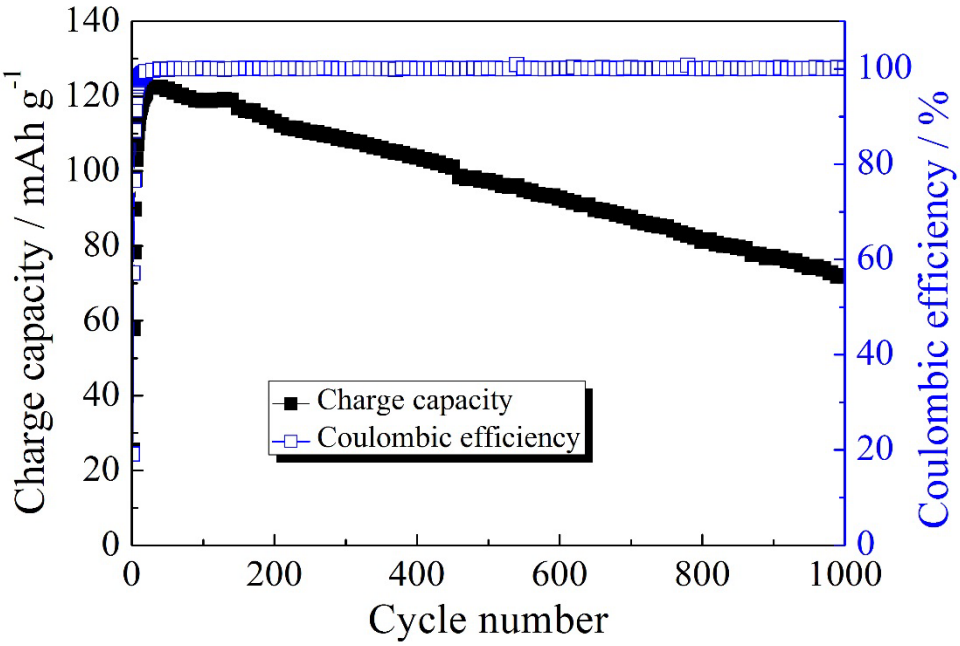

Figure S6. Cycling performance of TiO_2 electrode at current rate of 200 mA g^{-1} at 363 K.